This article was downloaded by:
On: *25 January 2011*
Access details: *Access Details: Free Access*
Publisher *Taylor & Francis*
Informa Ltd Registered in England and Wales Registered Number: 1072954 Registered office: Mortimer House, 37-41 Mortimer Street, London W1T 3JH, UK

Separation Science and Technology

Publication details, including instructions for authors and subscription information:
http://www.informaworld.com/smpp/title~content=t713708471

Absorption of Carbon Dioxide into Aqueous Solution of Sodium Glycinate

Sang-Wook Park[a]; Young-Sik Son[a]; Dae-Won Park[a]; Kwang-Joong Oh[a]
[a] Division of Chemical Engineering, Pusan National University, Busan, Korea

Online publication date: 22 June 2010

To cite this Article Park, Sang-Wook , Son, Young-Sik , Park, Dae-Won and Oh, Kwang-Joong(2008) 'Absorption of Carbon Dioxide into Aqueous Solution of Sodium Glycinate', Separation Science and Technology, 43: 11, 3003 — 3019

To link to this Article: DOI: 10.1080/01496390802219620

URL: http://dx.doi.org/10.1080/01496390802219620

PLEASE SCROLL DOWN FOR ARTICLE

Full terms and conditions of use: http://www.informaworld.com/terms-and-conditions-of-access.pdf

This article may be used for research, teaching and private study purposes. Any substantial or systematic reproduction, re-distribution, re-selling, loan or sub-licensing, systematic supply or distribution in any form to anyone is expressly forbidden.

The publisher does not give any warranty express or implied or make any representation that the contents will be complete or accurate or up to date. The accuracy of any instructions, formulae and drug doses should be independently verified with primary sources. The publisher shall not be liable for any loss, actions, claims, proceedings, demand or costs or damages whatsoever or howsoever caused arising directly or indirectly in connection with or arising out of the use of this material.

Separation Science and Technology, 43: 3003–3019, 2008
Copyright © Taylor & Francis Group, LLC
ISSN: 0149-6395 print/1520-5754 online
DOI: 10.1080/01496390802219620

Absorption of Carbon Dioxide into Aqueous Solution of Sodium Glycinate

Sang-Wook Park, Young-Sik Son, Dae-Won Park, and Kwang-Joong Oh
Division of Chemical Engineering, Pusan National University, Busan, Korea

Abstract: Carbon dioxide was absorbed into aqueous solution of sodium glycinate (SG) at different SG concentrations, CO_2 partial pressures, and temperatures in the range of 0.5–3.0 kmol/m^3, 25–101.3 kPa, and 298–318 K, respectively, using a stirred semi-batch vessel with a planar gas-liquid interface. Both the reaction order and rate constant are determined from gas absorption rates under the fast reaction regime. The reaction was found to be first order with respect to both CO_2 and SG. The activation energy for the CO_2-SG reaction has been found to be 59.8 kJ/mol. The second-order reaction rate constants were used to obtain the theoretical values of absorption rate based on the film theory.

Keywords: Absorption, carbon dioxide, sodium glycinate

INTRODUCTION

Carbon dioxide in the flue gas generated as a result of combustion of fossil fuel in thermal power plants, etc., is the main cause of global environmental problems such as air pollution and acid rain. One of the conventional methods to achieve the removal and recovery of CO_2 on an industrial scale is the chemical absorption method. One important requirement involved with this method is to develop absorbents with high absorption rate and capacity. Industrially important chemical absorbents are alkanolamines such as monoethanolamine, diethanolamine, *N*-methyldiethanolamine, and di-2-propanolamine (1).

Received 14 November 2007; accepted 15 April 2008.

Address correspondence to Sang-Wook Park, Division of Chemical Engineering, Pusan National University, Busan 609-735, Korea. E-mail: swpark@pusan.ac.kr

The kinetics of the reaction between CO_2 and alkanolamine was analyzed using simple mass balances which resulted from the zwitterion mechanism proposed by Danckwerts (2). Some discrepancies remained according to the reaction mechanism (3), kind of amines, gas/liquid contactor, and analysis method about the rate data, i.e., the order of the overall reactions and the rate constants. Recently, a group of so-called sterically hindered amines have been developed (4), because of high capacity of CO_2 per 1 mole of amine and relatively high absorption rate even at high CO_2 loading.

Amino acid or salts of amino acids are also reported to be used for the selective removal of acid gases in some industrial processes (5) as a new absorbent for CO_2 absorption, because of high surface tension, nonvolatile nature, resistance to degradation in oxygen-rich flue gas, and better absorption (6). Many studies have been done towards the mechanisms and kinetics of the reaction of CO_2 with various alkanolamines (1), whereas data about reaction kinetics of CO_2 with salt of amino acid are scarce (7,8). Lee et al. (6,8) have measured diffusivity and Henry's constant of CO_2 in aqueous solution of SG by N_2O analogy and obtained the reaction rate constant in CO_2-SG reaction under condition of an assumed pseudo-first order reaction. They did not observe the reaction order with respect to both CO_2 and SG.

In this paper, the experimental data about the absorption of CO_2 into aqueous solution of SG at 298–318 K using a stirred semi-batch vessel with a planar gas-liquid interface are presented. To investigate the reaction kinetics, measurements of the absorption rates have been done at different partial pressure of CO_2 and concentration of SG. Diffusivity and solubility of CO_2, which Lee et al. (8) have measured by N_2O analogy, are used to analyze the reaction order with respect to CO_2 and SG and reaction rate constant.

THEORY

In case of CO_2 absorption into aqueous solution containing primary and secondary amines, the zwitterions mechanism originally proposed by Caplow (9) and reintroduced by Danckwerts (2) and da Silva and Svendsen (3) is generally accepted to occur in two steps as follows:

$$CO_2(g) + RNH_2 = RN^+H_2COO^- \tag{i}$$

$$RN^+H_2COO^- + H_2O = RNH_3^+ + HCO_3^- \tag{ii}$$

It has been reported (10) that the first step in above two steps, the formation of the zwitterions, is slow and hence the rate-determining step is given by

$$CO_2(A) + RNH_2(B) + H_2O \rightarrow RNH_3^+ + HCO_3^- \qquad \text{(iii)}$$

Reaction (iii) may be formulated as follows:

$$A + \nu_A B \rightarrow \text{products} \qquad \text{(iv)}$$

where ν_A is a stoichiometric coefficient of species A and assumed to be 1 according to reaction (iii).

The following assumptions are made to set up the mass balance of species A and B:

1. Henry's law holds,
2. isothermal condition prevails, and
3. species B is a nonvolatile solute,
4. the gas-phase resistance to gas absorption is negligible, and
5. reaction (iv) is mth order with respect to A and nth order with respect to B, of which the reaction rate (r_A) is expressed by

$$r_A = k_2 C_A^m C_B^n \qquad \text{(v)}$$

The mass balances of species A and B in the film liquid based on the film theory accompanied by reaction (v) and the boundary conditions are given as follows:

$$D_A \frac{d^2 C_A}{dz^2} = k_2 C_A^m C_B^n \qquad (1)$$

$$D_B \frac{d^2 C_B}{dz^2} = \nu_A k_2 C_A^m C_B^n \qquad (2)$$

$$z = 0; \; C_A = C_{Ai}, \; \frac{dC_B}{dz} = 0 \qquad (3)$$

$$z = \delta; \; C_A = 0, C_B = C_{B_o} \qquad (4)$$

The molar flux of species A at the gas-liquid interface phase is defined by

$$N_A = -D_A \left(\frac{dC_A}{dz} \right)_{z=0} \qquad (5)$$

Because not only the physicochemical properties, but m and n should be given to obtain the theoretical N_A of Eq. (5), for the sake of convenience the systems may be classified into four regimes such as very slow reaction, slow reaction, fast reaction, and instantaneous reaction (11) depending on the relative rates of diffusion and reaction by using the dimensionless groups listed below.

The condition for validity of fast pseudo-mth-order reaction with respect to species A, where the interfacial concentration of species B is the same as that in the bulk liquid phase, is given by the following expression (11):

$$3 < \mathrm{Ha} < \mathrm{Ei} \tag{6}$$

where

$$Ha = \frac{\sqrt{\frac{2}{m+1} D_A k_2 C_{Ai}^{m-1} C_{Bo}^{n}}}{k_L} \tag{7}$$

$$Ei = \sqrt{\frac{D_A}{D_B}} + \frac{C_{Bo}}{\nu_A C_{Ai}} \sqrt{\frac{D_A}{D_B}} \tag{8}$$

Ei is defined as the instantaneous reaction enhancement factor and is derived from the penetration theory, since the experimental data of the absorption rates are better correlated through use of $(D_A/D_B)^{0.5}$ than D_A/D_B (11).

If Eq. (6) is satisfied, Eq. (1) can be written as

$$D_A \frac{d^2 C_A}{dz^2} = k_2 C_A^m C_{Bo}^n = k_m C_A^m \tag{9}$$

where

$$k_m = k_2 C_{Bo}^n \tag{10}$$

Using the solution of Eq. (9) with the boundary conditions of Eq. (3) and (4), N_A of Eq. (5) is derived as follows:

$$N_A = C_{Ai} \sqrt{\frac{2}{m+1} D_A k_2 C_{Ai}^{m-1} C_{Bo}^{n}} \tag{11}$$

Equation (11) shows that N_A is independent of k_L, that is, the hydrodynamics of the stirred semi-batch tank with a planar gas-liquid interface.

Where the resistance in the gas phase is not negligible, the expression for N_A for the pseudo-mth order regime is derived as follows:

$$\frac{P_A}{N_A} = \frac{1}{k_G} + \frac{H_A}{\sqrt{\frac{2}{m+1} D_A k_2 C_{Ai}^{m-1} C_{Bo}^{n}}} \tag{12}$$

For negligible resistance in the gas phase, plots of P_A/N_A vs. $H_A/(D_A k_2 C_{Bo})^{0.5}$ at constant temperature should, according to Eq. (12), be a straight line passing through the origin with slope of 1 for $m = n = 1$.

If both m and n are 1, the dimensionless forms of Eq. (1), (2), and the boundary conditions are very convenient to obtain the value of N_A as follows:

$$\frac{d^2a}{dx^2} = Mab \tag{13}$$

$$\frac{d^2b}{dx^2} = r_{AB} m_A Mab \tag{14}$$

$$x = 0;\ a = 1,\ db/dx = 0 \tag{15}$$

$$x = 1;\ a = 0,\ b = 1 \tag{16}$$

where
$a = C_A/C_{Ai}, b = C_B/C_{Bo}, x = z/z_L, M = k_2 C_{Bo} D_A/k_L^2, m_A = \nu_A C_{Ai}/C_{Bo}$, $r_{AB} = D_A/D_B$

The enhancement factor (β) here defined as the ratio of molar flux of Eq. (5) with chemical reaction to that obtained without chemical reaction:

$$\beta = -\left.\frac{da}{dx}\right|_{x=0} \tag{17}$$

The solution of Eq. (13) and (14) is used to obtain the value of β through Eq. (17).

EXPERIMENTAL

All chemicals were of reagent grade, and used without further purification, Purity of CO_2, and N_2 were more than 99.9%.

Absorption experiments were carried out in an agitated vessel. The absorption vessel was constructed of glass of 0.073 m in inside diameter and of 0.151 m in height. Four equally spaced vertical baffles, each one-tenth of the vessel diameter in width, were attached to the internal wall of the vessel. The gas and liquid phase were agitated with an agitator driven by a 1/4 Hp variable speed motor. Two straight impellers with 0.034 m in length and 0.05 m in width were used as the agitators in gas and liquid phase, respectively, which were agitated at the middle position of each phase with the agitation speed of 50 rpm. The surface area of the

Table 1. Absorption data for various SG concentrations and CO_2 partial pressures at 298 K

C_{Bo} (kmol/ m^3)	$D_A \times 10^9$ m^2/s)	P_A (kPa)	$C_{Ai} \times 10^3$ (kmol/ m^3)	$N_{Ae} \times 10^6$ (kmol/ m^2s)	$N_{Ae}{}^2/$ $C_{Ai}{}^2D_A$ (1/s)	$k_L \times 10^6$ (m/s)	Ha	Ei
1	1.485	25.83	0.82	3.61	131	5.35	83	244
		48.52	1.54	6.78	131	6.44	69	131
		79.01	2.50	11.00	130	7.00	63	81
		101.30	3.21	14.09	130	7.54	59	64
2	1.391	25.83	0.79	4.77	260	5.64	107	501
		48.12	1.48	8.87	258	6.90	88	270
		74.86	2.30	14.00	266	7.74	78	174
		101.30	3.11	18.86	264	8.17	74	129
3	1.298	26.84	0.80	5.68	390	6.07	118	747
		50.04	1.49	10.62	393	7.28	98	401
		76.08	2.26	16.19	395	8.22	87	265
		101.30	3.01	21.59	396	8.93	80	199

liquid was measured and its value was $4.10 \times 10^{-3}\,m^2$. The value of the cumulative volume of the soup bubble was measured by a soup bubbler for the change of absorption time to obtain the absorption rate of CO_2. It was assumed that the volumetric rising rate of the soup bubble in the soup bubbler attached to the absorption vessel was equal to the value

Table 2. Absorption data for various SG concentrations and CO_2 partial pressures at 308 K

C_{Bo} (kmol/ m^3)	$D_A \times 10^9$ (m^2/s)	P_A (kPa)	$C_{Ai} \times 10^3$ (kmol/ m^3)	$N_{Ae} \times 10^6$ (kmol/ m^2s)	$N_{Ae}{}^2/$ $C_{Ai}{}^2D_A$ (1/s)	$k_L \times 10^6$ (m/s)	Ha	Ei
1	1.808	26.64	0.69	4.74	264	5.74	122	263
		49.13	1.27	8.84	269	7.04	100	144
		78.61	2.03	14.11	268	7.76	91	95
		101.30	2.61	18.16	267	8.28	85	89
2	1.66	25.43	0.63	6.01	541	5.73	166	568
		49.43	1.23	11.66	539	7.31	130	293
		75.87	1.89	17.87	537	7.85	121	192
		101.30	2.53	23.84	536	8.33	114	144
3	1.516	25.43	0.61	6.79	811	5.77	193	882
		50.95	1.23	13.57	808	7.81	143	441
		75.87	1.83	20.00	791	8.69	128	297
		101.30	2.44	27.05	812	9.56	117	223

Table 3. Absorption data for various SG concentrations and CO_2 partial pressures at 318 K

C_{Bo} (kmol/m^3)	$D_A \times 10^9$ (m^2/s)	P_A (kPa)	$C_{Ai} \times 10^3$ (kmol/m^3)	$N_{Ae} \times 10^6$ (kmol/m^{2}s)	$N_{Ae}^2/C_{Ai}^2 D_A$ (1/s)	$k_L \times 10^6$ (m/s)	Ha	Ei
1	2.178	26.64	0.56	6.36	599	6.33	181	295
		49.94	1.04	11.65	571	6.99	164	258
		76.48	1.60	18.07	586	8.41	136	204
		101.3	2.12	24.12	595	8.34	130	179
2	1.947	26.14	0.53	8.08	1188	6.83	224	618
		48.93	0.99	15.05	1176	7.49	204	331
		80.53	1.64	24.75	1174	8.15	188	202
		101.3	2.06	31.20	1180	8.51	180	191
3	1.748	25.73	0.50	8.74	1730	7.01	253	979
		50.14	0.98	17.48	1822	7.76	229	503
		76.58	1.50	26.23	1758	8.78	202	330
		101.3	1.98	34.97	1786	9.21	193	2504

Table 4. Absorption data for various SG concentrations at $P_A = 101.3$ kPa

Temp (K)	C_{Bo} (kmol/m^3)	$D_A \times 10^9$ (m^2/s)	C_{Ai} (kmol/m^3)	$N_{Ae} \times 10^6$ (kmol/m^{2}s)	$N_a^2/C_{Ai}^2 D_A$ (1/s)	$k_2 C_{Bo}$	Ha	Ei
298	0.46	1.536	0.0325	9.725	58	61	40	49
	1.00	1.485	0.0321	14.25	133	132	59	62
	1.50	1.438	0.0316	17.41	211	198	72	95
	2.03	1.388	0.0311	19.52	284	268	85	130
	2.52	1.342	0.0306	20.18	324	332	95	164
	3.03	1.295	0.0301	21.29	386	400	105	200
308	0.51	1.882	0.0265	13.50	562	139	60	70
	1.00	1.808	0.0261	18.31	603	273	85	91
	1.55	1.726	0.0257	21.73	654	422	106	109
	1.98	1.663	0.0253	24.15	699	540	121	141
	2.30	1.617	0.0250	25.94	735	627	131	166
	3.07	1.506	0.0243	27.27	835	837	153	227
318	0.53	2.298	0.0214	17.97	306	319	99	103
	1.00	2.178	0.0212	24.42	610	601	137	147
	1.45	2.070	0.0209	28.69	907	372	166	170
	1.97	1.954	0.0206	31.73	1214	1185	196	205
	2.48	1.848	0.0202	33.90	1519	1491	222	234
	3.05	1.739	0.0197	35.40	1848	1834	249	254

of absorption rate of CO_2. The measured molar flux of CO_2 (N_{Ae}) was obtained using the absorption rate and the surface area of the liquid. The absorption experiments were carried out in the range of 0.5–3.0 kmol/m^3 of SG, 25–101.3 kPa of CO_2 partial pressure, and 298–313 K along the procedure similar to those reported elsewhere (12,13). Viscosity of aqueous solution of SG was measured using Cannon-Fenske viscometer (Brookfield Eng. Lab. Inc, USA).

RESULTS AND DISCUSSION

The nitrous oxide analogy (8,14–18) has been used to approximate diffusivity and Henry's constant of gas species in aqueous solution. Song et al. (8) have measured diffusivity and Henry's constant (H_A) of CO_2 in aqueous solution of SG in the SG concentration range of 1–3.5 kmol/m^3 and 303–323 K using N_2O analogy. In this study, the data of D_A and H_A measured by Lee et al. (8) are used to obtain the empirical formulae by non-linear minimization technique using Sigma plot program, which

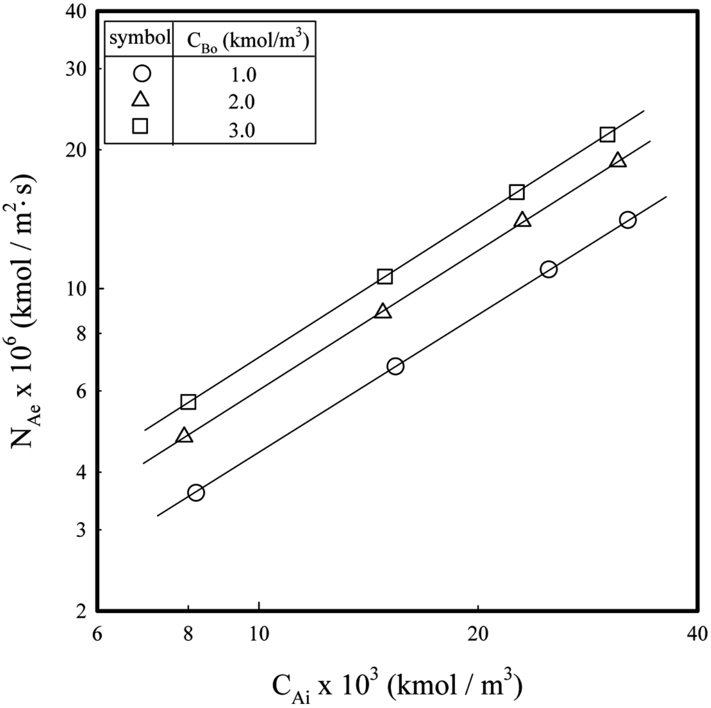

Figure 1. Effect of C_{Ai} on N_{Ae} at different concentrations of SG at 298 K.

are expressed as function of SG concentration at each temperature of 298, 308, and 313 K as follows:

$$\text{For 298 K}, D_A = [-4.2072 + 5.7879 \times \text{Exp}(-0.0167 \times C_{Bo})] \times 10^{-9} \tag{18}$$

$$\text{For 308 K}, D_A = [-4.1556 + 6.1153 \times \text{Exp}(-0.0251 \times C_{Bo})] \times 10^{-9} \tag{19}$$

$$\text{For 318 K}, D_A = [-0.4949 + 1.959 \times \text{Exp}(-0.1473 \times C_{Bo})] \times 10^{-9} \tag{20}$$

$$\text{For 298 K}, H_A = 2618.25 + 461.14 \times \text{Exp}(0.1597 \times C_{Bo}) \tag{21}$$

$$\text{For 308 K}, H_A = 2857.0 + 906.4 \times \text{Exp}(0.1196 \times C_{Bo}) \tag{22}$$

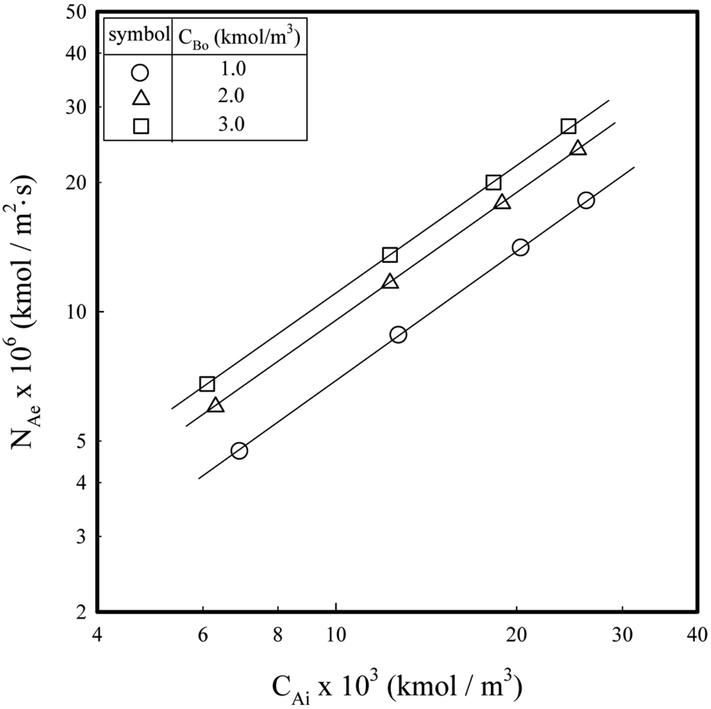

Figure 2. Effect of C_{Ai} on N_{Ae} at different concentrations of SG at 308 K.

$$\text{For } 318\,\text{K}, H_A = 4454.0 + 230.2 \times \text{Exp}(0.3535 \times C_{Bo}) \tag{23}$$

D_B is estimated from Wilke-Chang equation (19).

The solubility (C_{Ai}) of CO_2 of a given partial pressure of CO_2 in aqueous solution of a given concentration of SG was estimated as follows:

$$P_A = H_A C_{Ai} \tag{24}$$

The values of D_A and C_{Ai}, and N_{Ae} at different C_{Bo}, P_A, and T are listed in Table 1–4.

To determine the order with respect to CO_2, logarithmic plots of N_{Ae} vs. C_{Ai} at different C_{Bo} in the range of 1–3 kmol/m^3 are shown in Fig. 1–3 using data presented in Table 1–3.

These plots are linear (correlation coefficient > 0.999) with a slope of unity in each C_{Bo}. This, according to Eq. (11), indicates that the order with respect to CO_2 is 1.

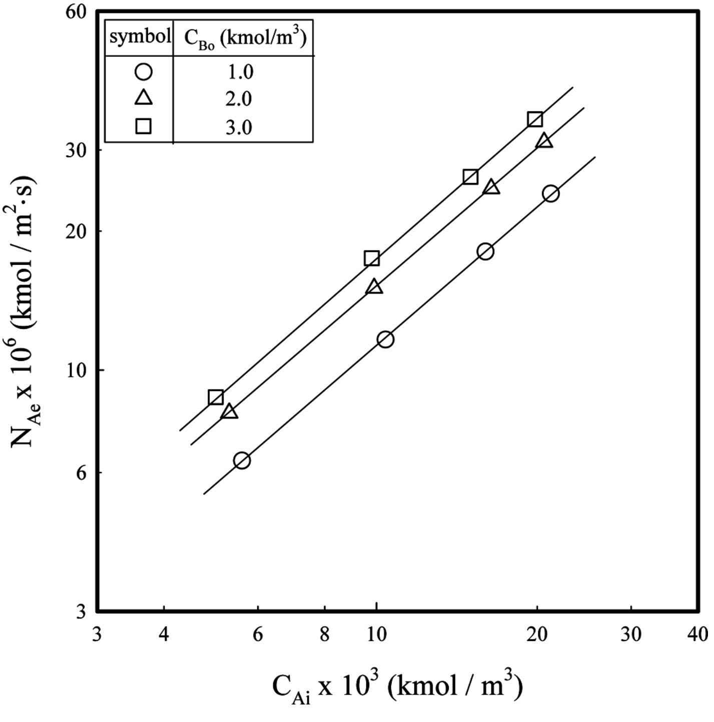

Figure 3. Effect of C_{Ai} on N_{Ae} at different concentrations of SG at 318 K.

To determine the order with respect to the concentration of SG, logarithmic plots of $(N_{Ae}/C_{Ai}D_A{}^{0.5})$ vs. C_{Bo} at different temperatures in the range of 298–318K are shown in Fig. 4 using the data presented in Table 4.

Each of these plots as shown in Fig. 4 is a straight line (correlation coefficient >0.999) with a slope of 1. This, according to Eq. (11), indicates that the order with respect to SG is 1.

The values of the reaction rate constant have been found out from the intercept of the plots of data in Fig. 4. The second order rate constant has been found to be 132, 273, 601 $m^3/kmol \cdot s$ at 298, 308, 318 K, respectively, and are listed in Table 5. Figure 5 shows the Arrhenius plots of the values of the reaction rate constant of CO_2-SG at different temperatures using data mentioned above.

Linear regression analysis of the Arrhenius plots leads the following expression for k_2 (correlation coefficient = 0.998).

$$k_2 = 3.82 \times 10^{12} \mathrm{Exp}(-7188/T) \tag{25}$$

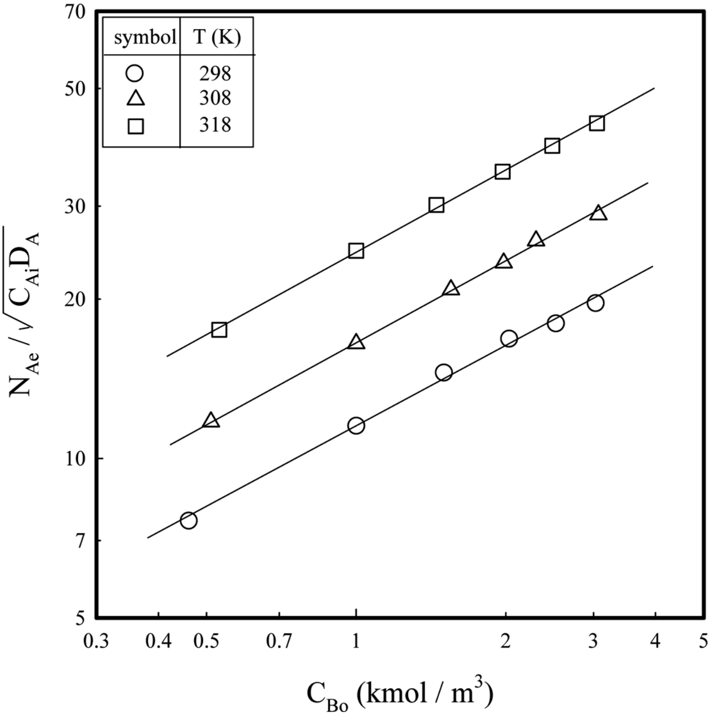

Figure 4. Logarithmic plots of $N_{Ae}/C_{Ai}D_A{}^{0.5}$ vs. C_{Bo} at various temperatures.

Table. 5. Reaction rate constant for CO_2–SG reaction at different temperatures

T (K)	k_2 (m^3/kmol · s)	k_2 (m^3/kmol · s) (8)
298	132	131
308	273	302
318	601	661

The corresponding value of the activation energy has been calculated to be 59.8 kJ/mol.

Lee et al. (8) have investigated the kinetics of the CO_2-SG reaction using a wetted wall column in the temperature range of 303–323 K and SG concentration of 1–3.5 kmol/m^3. Theyhave obtained the activation energy of 63.8 kJ/mol and the second order rate constant using a reaction regime of the pseudo-first-order with respect to CO_2 as follows:

$$k_2 = 1.95 \times 10^{13} \mathrm{Exp}(-7670/T) \tag{26}$$

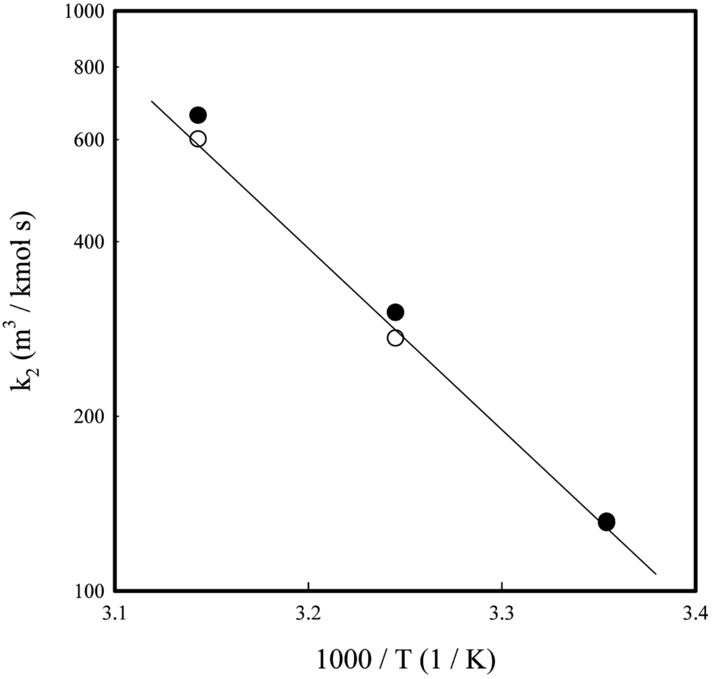

Figure 5. Arrhenius plots for CO_2-SG reaction with the filled circles from Lee et al. (8).

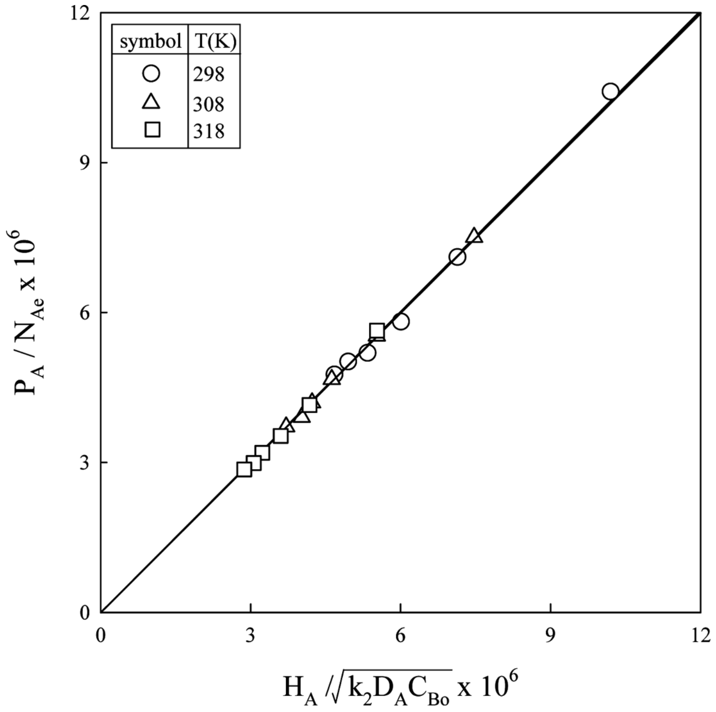

Figure 6. Plots of P_A/N_{Ae} vs $H_A/(k_2D_AC_{Bo})^{0.5}$ at various temperatures.

They measured the diffusivity and Henry constant by N_2O analogy and assumed that the reaction was first order with respect to both CO_2 and SG, but did not ensure the reaction order experimentally. The values of the second order rate constant calculated using Eq. (26) are shown in Fig. 5 and Table 5. As shown in Table 5, the second order rate constants in this study are in agreement with those by Lee et al. (8).

To ensure that the gas phase resistance was really negligible in all run, plots of P_A/N_{Ae} vs. $H_A/(k_2D_AC_{Bo})^{0.5}$ at different temperatures have been made following Eq. (12) for $m = 1$, $n = 1$ using relevant data from Table 1–3. The corresponding values of H_A and D_A have been estimated using Eq. (18)–(23). These plots are presented in Fig. 6.

It can be seen from Fig. 6 that all plots of P_A/N_{Ae} vs. $H_A/(k_2D_AC_{Bo})^{0.5}$ are straight lines with slope of 1 and passing through the origin. This, according to Eq. (12), signifies negligible gas phase resistance.

The concentrations of CO_2 and SG in the liquid film are obtained from the numerical solution of Eqs. (13) and (14) using the finite element method by FEMLAB soft program with the dimensionless parameters (r_{AB}, M, m_A) containing the values of k_2, D_A, D_B, C_{Ai}, and k_L, At the

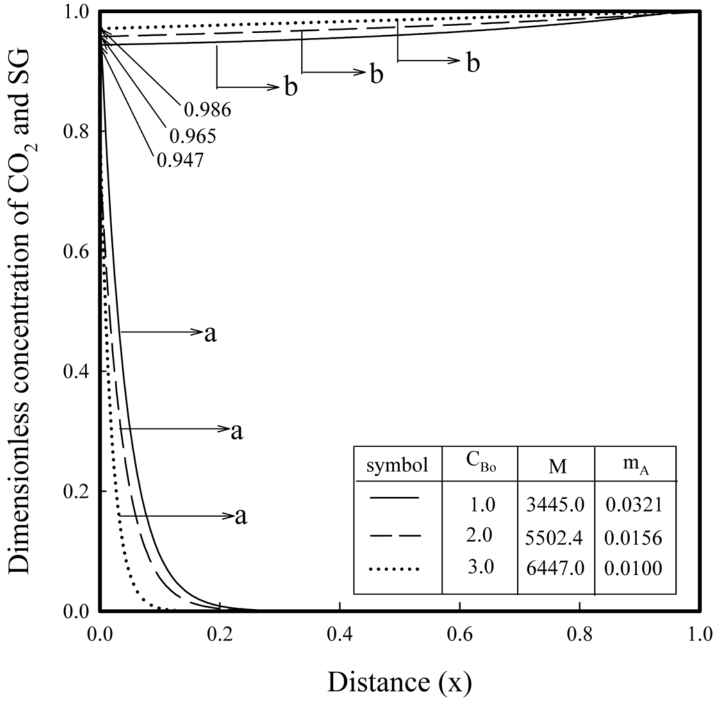

Figure 7. Dimensionless concentration profiles of CO_2 and SG in the liquid film at $P_A = 101.3\,\text{kPa}$, $r_{AB} = 0.2547$, and 298 K for different C_{Bo}. ($a = C_A/C_{Ai}$, $b = C_B/C_{Bo}$).

typical condition of $P_A = 101.3\,\text{kPa}$ and 298 K, the dimensionless concentration profiles of CO_2 and SG in the liquid film are illustrated for various C_{Bo} of 1, 2 and $3\,\text{kmol/m}^3$, respectively, in Fig. 7.

The dimensionless parameters at the typical condition are listed in Fig. 7. As shown in Fig. 7, C_A decreases and C_B increases with increasing the depth of the liquid film (x), and the slope of the concentration profile of CO_2 at the gas-liquid interface increase with increasing C_{Bo}, which make N_{Ae} increased as shown in Table 1–4. The values of C_B at the gas-liquid interface increase with increasing C_{Bo} and all of them are above 0.94. This means that C_B may be constant as C_{Bo} at this typical condition. The values of Ha and Ei at $m = n = 1$ are calculated by Eq. (7) and (8), and listed in Table 1–4. As shown Table 1–4, Eq. (6) is satisfied. Therefore, the reaction between CO_2 and SG may be a fast pseudo-first-order reaction regime.

The enhancement factor is estimated by Eq. (17) using the concentration profile of A, which is obtained from the solution of Eq. (13)

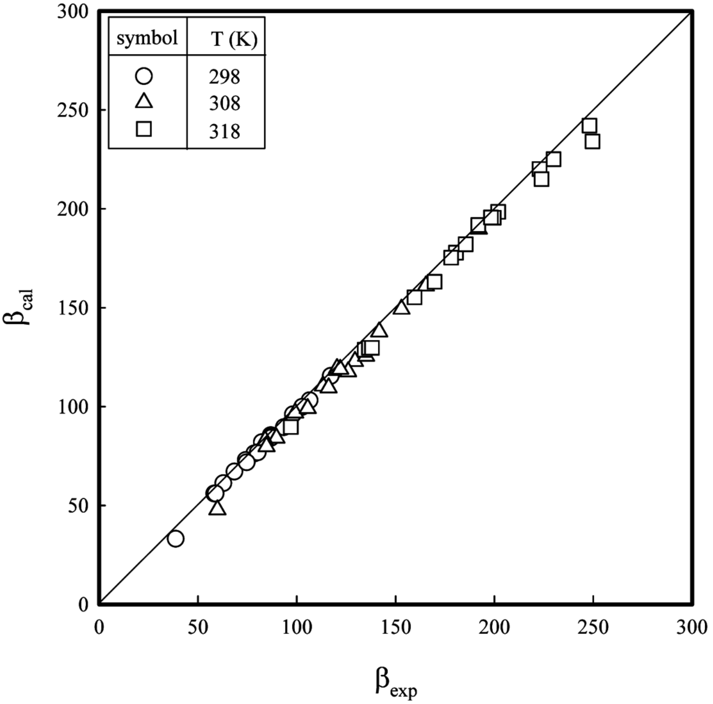

Figure 8. Comparison of estimated enhancement factors of CO_2 with observed ones. (C_{Bo}: 0.5–3.0 kmol/m^3, P_A: 25–101.3 kPa, T: 298–313 K).

and (14). The comparison of observed and estimated enhancement factors in the SG concentration range of 0.5–3.0 kmol/m^3, 25–101.3 kPa of CO_2 partial pressure, and 298–313 K is shown in Fig. 8.

As shown in Fig. 8, the observed values of the enhancement factors agree with the estimated values (correlation coefficient = 0.9695).

To confirm reliability of the experimental data, $N_{Ae}^2/(C_{Ai}^2 D_A)$ are listed in Table 1–4 and $k_2 C_{Bo}$ in Table 4. As show in Table 1–3, the values of $N_{Ae}^2/(C_{Ai}^2 D_A)$ are almost same one another at fixed C_{Bo} and, as shown in Table 4, those are almost equal to $k_2 C_{Bo}$ each other. These results, according to Eq. (11) for m = n = 1, indicate that the experimental data may be reasonable.

CONCLUSIONS

The reaction kinetics between CO_2 and SG have been investigated at different temperatures in the range of 298–318 K using a stirred semi-batch vessel with a planar gas-liquid interface. The reaction has been found to be first order with respect to both CO_2 and SG. The second order rate constants have been determined as 132, 273, 601 m^3/kmolñs at 298, 308, 318 K, respectively, within SG concentration range of 0.5–3 kmol/m^3. The activation energy for the CO_2-SG reaction has been found to be 59.8 kJ/mol. The second order rate constants are in agreement with those by Lee et al. (8), who used a different absorber and method for analyzing the absorption data.

NOMENCLATURE

C_i: concentration of species, i (kmol/m^3)
D_i: diffusivity of species, i (m^2/s)
Ei: instantaneous reaction enhancement factor define in Eq. (8)
Ha: Hatta number defined in Eq. (7)
H_A: Henry constant of CO_2 (m^3·kP$_A$/kmol)
k_G: gas phase mass transfer coefficient of CO_2 (m^2·s·kP$_A$/kmol)
k_L: liquid-side mass transfer coefficient of CO_2 in absorbent (m/s)
k_m: pseudo mth order reaction rate constant in Eq. (9) (1/s)
k_2: second-order reaction rate constant in reaction (iv) (m^3/kmol·s)
m: reaction order with respect to CO_2
n: reaction order with respect to SG
P_A: partial pressure of CO_2 (kPa)
N_A: molar flux of CO_2 defined in Eq. (5) (kmol/m^2·s)
N_{Ae}: experimental molar flux of CO_2 (kmol/m^2·s)
r_A: reaction rate defined in Eq. (v)
SG: sodium glycinate
T: temperature (K)
z: diffusion coordinate of CO_2 (m)

Greek Letters

β: enhancement factor of CO_2 defined in Eq. (17)
δ: liquid film thickness (m)

Subscripts

A: CO_2
B: SG
i: gas-liquid interface
o: feed

ACKNOWLEDGEMENTS

This work was supported with Brain Korea project. Dae-Won Park is also grateful to KOSEF (R01-2007-000-10183-0).

REFERENCES

1. Astarita, G.; Savage, D.W.; Bisio, A. (1983) *Gas Treating with Chemical Solvents*; John Wiley & Sons: New York.
2. Danckwerts, P.V. (1979) The reaction of CO_2 in ethanolamines. *Chem. Eng. Sci.*, *34*: 443–446.
3. da Silva, E.F.; Sendsen, H.F. (2004) Ab initiol study of the reaction of carbamate formation from CO_2 and alkanolamine. *Ind. Eng. Chem. Res.*, *43*: 3413–3418.
4. Mimura, T.; Suda, T.; Honda, A.; Kumazawa, H. (1998) Kinetics of reaction between carbon dioxide and sterically hindered amines for carbon dioxide recovery from power plant flue gases. *Chem. Eng. Commun.*, *170*: 245–260.
5. Kohl, A. L.; Nielson, R. B. (1997) *Gas Purification*; Gulf Publishing: Houston.
6. Lee, S.; Song, H.J.; Maken, S.; Shin, H.C.; Park, J.W. (2006) Physical solubility and diffusivity of N_2O and CO_2 in aqueous sodium glycinate solutions. *J. Chem. Eng. Data*, *51*: 504–509.
7. Chen, H.; Kovvali, A.S.; Sirkar, K.K. (2000) Selective CO_2 separation from CO_2-N_2 mixtures by immobilized glycine-Na-glycerol membranes. *Ind. Eng. Chem. Res.*, *39*: 2447–2451.
8. Lee, S.; Song, H.J.; Maken, S.; Park, J.W. (2007) Kinetics of CO_2 absorption in aqueous sodium glycinate solutions. *Ind. Eng. Chem. Res.*, *46*: 1578–1583.
9. Caplow, M. (1968) Kinetics of carbamate formation and breakdown. *J. Am. Chem. Soc.*, *90*: 6795–6803.
10. Yih, S.M.; Shen, K.P. (1988) Kinetics of carbon dioxide reaction with srerically hindered 2-amino-2-methyl-1-propanol. *Ind. Eng. Chem. Res.*, *27*: 2237–2241.
11. Daraiswany, L.K.; Sharma, M.M. (1984) *Heterogeneous Reaction: Analysis, Example and Reactor Design*; John Wiley & Sons: New York.
12. Yu, W.C.; Astarita, G.; Savage, D.W. (1985) Kinetics of carbon dioxide absorption in solutions of methyldiethanolamine. *Chem. Eng. Sci.*, *40*: 1585–1590.
13. Park, S.W.; Choi, B.S.; Song, K.W.; Oh, K.J.; Lee, J.W. (2007) Absorption of carbon dioxide into aqueous xanthan gum solution containing monoethanolamine. *Sep. Sci. Technol.*, *42*: 3537–3554.
14. Versteeg, G.F.; van Swaaij, W.P.M. (1988) Solubility and diffusivity of acids gases (CO_2, N_2O) in aqueous alkanolamine solutions. *J. Chem. Eng. Data*, *33*: 29–34.
15. Pasiuk-Bronikowska, W.; Rudzinski, K.J. (1991) Absorption of SO_2 into aqueous systems. *Chem. Eng. Sci.*, *46*: 2281–2291.
16. Totiwachwuthikul, P.; Meisen, A.; Lim, C.J. (1991) Solubility of CO_2 in 2-amino-2–methyl-1-propanol solutions. *J. Chem. Eng. Data*, *36*: 130–133.
17. Wang, Y.W.; Xu, S.; Otto, F.D.; and Mather, A.E. (1992) Solubility of N_2O in alkanolamines and in mixed solvents. *Chem Eng. J.*, *48*: 31–40.
18. Saha, A.K., Bandyopadhyay, S.S.; and Biswas, A.K. (1993) Solubility and diffusivity of N_2O and CO_2 in aqueous solutions of 2-amino-methyl-1-propanol. *J. Chem. Eng. Data*, *38*: 78–82.
19. Danckwerts, P.V. (1970) *Gas-Liquid Reactions*; McGraw-Hill: New York.